New challenges for adaptive optics: the OWL 100m telescope

N. Hubin, M. Le Louarn, M. Sarazin, A. Tokovinin, E. Viard

European Southern Observatory
Karl Schwarzschild str., 2 D-85748 Garching bei München Germany

ABSTRACT

Adaptive optics will be a key element of future Extremely Large Telescopes (ELTs) which need sharp images both to avoid object confusion and to boost sensitivity to point sources against sky background. A challenging task of correcting turbulence in the visible part of the spectrum is addressed. With an R $\sim$ 10 natural guide star a Strehl ratio (SR) of 0.6 can be achieved at 500 nm, at the cost of an extremely low sky coverage. Thus, use of Multi-Conjugate Adaptive Optics techniques will be essential to widen the field of view (FOV). We summarize our recent theoretical results and show that with 3 deformable mirrors it is realistic to obtain a FOV diameter of $30''$–$60''$ in the visible, or $3'$–$6'$ in the K band. Contrary to the common belief, the layered structure of the turbulence vertical profile is not needed to achieve this limit, neither do we need to know the profile exactly.

The wide corrected FOV ensures a reasonably good sky coverage in the near infrared using 4 natural guide stars (60% in the J band at medium Galactic latitudes). Artificial Laser Guide Stars will be needed to correct in the visible, using in addition a faint natural star to measure low-order wavefront aberrations. On ELTs this star can be faint, up to R=23, so a good sky coverage can also be obtained. A significant fraction of guide sources at these magnitudes are extragalactic.

Keywords: adaptive optics, multi-conjugate adaptive optics, large telescopes, isoplanatic angle, turbulence profiles

1. INTRODUCTION

The diameter of the primary mirror of current ground based optical telescopes is between 8 and 10 m. Proposals have arisen for the next generation of telescopes. The diameter of the primary lies between 30 m and 100 m (e.g.[1–3]). Adaptive optics (AO) in the visible part of the spectrum will certainly play a crucial role, since it provides the diffraction limit (1 milli-arcsecond for a 100 m telescope) which helps to prevent source confusion for extragalactic studies and reduces the background contribution. Competition with space-based observatories[4] is also a strong driver for AO on Extremely Large Telescopes (ELTs).

The goal of our study is to explore the fundamental limitations of a visible-light AO system on an ELT. We first model a Natural Guide Star (NGS) system, which provides a target Strehl ratio (SR) of 60 % in the visible. Since the sky coverage (in the visible) for such a solution is extremely small, we explore the performance of Multi-Conjugate Adaptive Optics (MCAO), which obtains a larger corrected FOV and an increased sky coverage by compensating the turbulence with several deformable mirrors conjugated to different heights. To do it, we need the 3D information on the instantaneous perturbation in the whole atmosphere, so MCAO is often associated with turbulence tomography. Using real turbulence profiles at the Paranal Observatory, the limiting FOV size is found. Taking into account this constraint, we investigate the sky coverage of a first generation AO system (optimized in the IR) based on several NGSs. Then we study the option of using multiple Laser Guide Stars (LGSs) for a second generation AO system, optimized for the visible. Both options promise a reasonably good sky coverage.

Send correspondence to NH
E-mail: NH: nhubin@eso.org
MLL: lelouarn@eso.org
MS: msarazin@eso.org
AT: atokovin@eso.org
EV: eviard@eso.org

Table 1. AO simulation parameters. Atmospheric values are given at 0.5 μm.

General parameters		Wavefront sensor	
Telescope diameter	100 m	Readout noise	1 e^-
Number of actuators	$\sim$ 500000	Peak quantum efficiency	90%
Transmission[1]	40%	Spectral bandwidth	500 nm
Seeing	0.5″	Sub-aperture size	16 cm
Coherence time	6 ms	Max. sampling rate	500 Hz
Isoplanatic angle	3.5″		

[1]Transmission of the atmosphere and telescope optics to the wavefront sensor. For visible light observations, light must be split between the wavefront sensor path and imaging path.

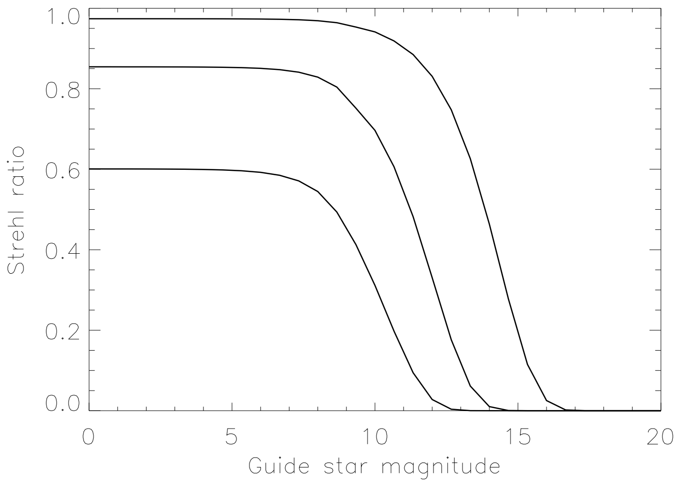

Figure 1. Strehl ratio versus magnitude at the wavelengths 2.2, 1.25 and 0.5 μm (from top curve to bottom) for one on-axis NGS with the telescope pointing at zenith

2. AO PERFORMANCE WITH AN ON-AXIS NGS

Using an analytical approach to compute AO performance,[5] we modeled a visible light AO system on a 100 m telescope. The system with a Shack-Hartmann sensor can be designed to provide a 60 % SR at 0.5 μm. This is higher than the SR needed to fulfill the scientific goal ($\sim$ 40%), to take into account potential error sources outside the AO system itself (e.g. optical aberrations or co-phasing errors of the segments of the primary mirror of the telescope).

We chose an atmospheric model corresponding to good observing conditions[5] at the Very Large Telescope observatory of Cerro-Paranal, Chile. The main atmospheric parameters are summarized in Table 1.

The effects of scintillation on the wavefront sensor and turbulence outer scale effects were not taken into account. The simulation results are presented in Fig. 1.

3. LIMITATIONS OF THE MCAO FIELD OF VIEW SIZE

The ultimate FOV size that can be compensated by MCAO is, evidently, of primary concern for ELTs because, apart from the size of the scientific FOV, it determines the sky coverage. First estimates of the tomographic FOV size were very optimistic, because it was supposed that all turbulence is concentrated in a few thin layers.[6] In this case the FOV is limited only by the beam overlap in the upper atmosphere, and increases in proportion to telescope diameter.

Real turbulence profiles, however, do not follow this idealistic model. Although the existence of strong thin layers is typical, there is always some turbulence in-between. It was not clear until recently to what extent the shape of realistic turbulence profiles limits tomographic techniques. This problem is actually under study by our group.[7,8] Our main results are summarized in this section.

Table 2. Profile data for Cerro Paranal and atmospheric parameters for a wavelength of 500 nm.

N	Flight	Date	Time	r_0, m	θ_0, $''$	θ_3, $''$	δ_5, m
1	38	10.03.92	3:30	0.32	3.80	28.88	463
2	39	11.03.92	4:45	0.15	4.09	26.86	235
3	40	12.03.92	1:30	0.21	3.58	24.51	411
4	43	14.03.92	2:45	0.07	0.42	5.70	581
5	45	15.03.92	1:00	0.19	2.05	16.29	491
6	46	15.03.92	5:00	0.22	1.74	15.13	655
7	48	16.03.92	4:10	0.17	2.48	17.23	406
8	50	24.03.92	8:12	0.13	1.66	17.17	378
9	51	25.03.92	2:43	0.26	2.03	21.74	572
10	52	25.03.92	7:11	0.21	2.22	17.09	526
11	54	23.03.92	4:10	0.22	2.81	19.63	474
12	55	29.03.92	9:15	0.14	1.65	8.78	549

Exploring fundamental limitations, we considered first an imaginary case when the instantaneous turbulence phase screens are exactly known in all layers, and investigated a quality of correction using only a few deformable mirrors (DMs). This *correction-limited* situation can be described by the isoplanatic angle θ_M – the limiting FOV radius which depends on turbulence altitude profile and the number of DMs. This generalizes the isoplanatic angle θ_0 of Fried[9] to the MCAO case.

But how well can we reconstruct the required correction signals from the wavefront measurements of several suitable guide sources, given the real turbulence profiles? The second limitation is related to *wavefront reconstruction* techniques. To study this limitation, an ideal case is again considered when several bright natural guide stars (NGS) are found around the FOV center. All problems of incomplete pupil overlap at high altitudes, spherical wavefronts and tilt indetermination when using LGS are left aside at this stage. The resulting error of object wavefront reconstruction depends only on the NGS configuration and the turbulence profile. This limiting error can be described by a new parameter δ – equivalent thickness of the atmosphere.

In the following sub-sections we review the properties of real turbulence profiles and estimate the parameters θ_M and δ which limit the MCAO FOV size. It is shown that correction is more restrictive than reconstruction, and that the layered distribution of turbulence is of no particular importance for MCAO, contrary to the current belief.

3.1. Turbulence profiles at Paranal

We have analyzed the PARSCA (Paranal Seeing Campaign[10]) balloon data on the vertical distribution of turbulence to test the assumption that all turbulence is concentrated within a few turbulent layers. During the site testing campaign, 12 balloons were launched at night time to measure the profile of variations of the refraction index constant, $C_n^2(h)$. SCIDAR (Scintillation Detection and Ranging[11]) measurements were also made simultaneously, confirming the balloon soundings.[12]

Table 2 summarizes some parameters of the balloon profiles. The average Fried parameter r_0 was 19 cm at 0.5 μm, corresponding to a seeing of $0.54''$ – slightly better than the average seeing at Paranal, $0.65''$. Considering the small time span during which the balloons were launched (19 days), these data are not fully representative of the site. The parameters have been corrected for the height difference between the observatory and the launching site, which explains the slight difference with other publications (e.g.[12]).

In Fig. 2 the cumulative distributions are plotted for an average of the 12 profiles and for the two selected profiles which have typical integral parameters r_0 and θ_0, but quite different shapes. Profile 51 has a strong layer at 7.5 km, apart from the ground layer which is present on all profiles. Even in this extreme case it can be seen that the cumulative distribution does not stay flat between these two layers, which account only for 2/3 of the total turbulence. The remaining 1/3 is distributed continuously. So, the assumption of thin discrete layers is evidently an over-simplification.

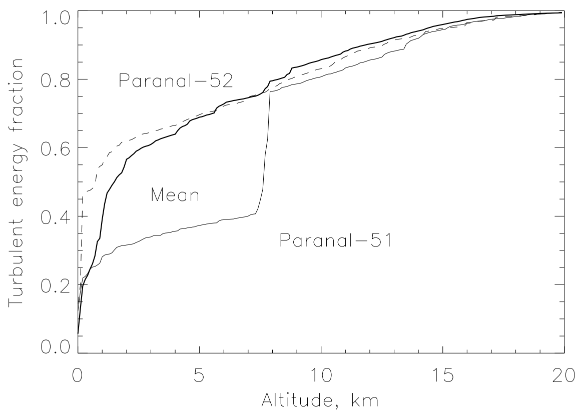

Figure 2. Cumulative distribution of turbulence at Paranal: fraction of total turbulent energy below a given altitude. The mean profile is plotted in thick line. Profile 52 (dotted line) is almost uniform above 2 km, while profile 51 (thin line) has a strong layer at 7.5 km above the site, containing about 1/3 of the total energy.

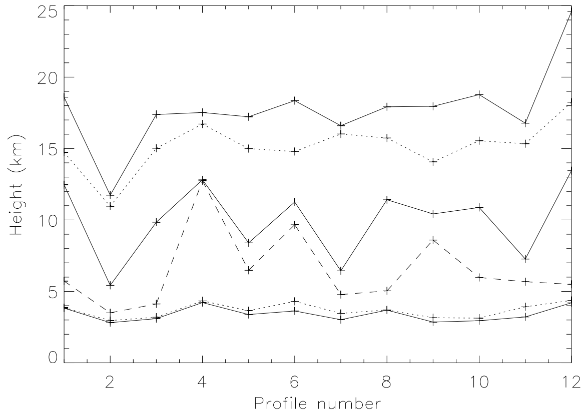

Figure 3. Optimized conjugate heights of the DMs (in km) as a function of profile number. Solid lines are for the 3 DM configuration, dots for the 2 DM configuration and dash is for a single DM.

3.2. Isoplanatic angle

The generalized isoplanatic angle θ_M in the sense of Fried[9] (i.e. corresponding to the 1 rad^2 phase variance) is expressed as[7]

$$\theta_M = \left[2.905 (2\pi/\lambda)^2 \int C_n^2(h) F_M(h, H_1, H_2, \cdots, H_M) \mathrm{d}h \right]^{-3/5}, \tag{1}$$

where F_M is a function depending on the conjugation heights of the DMs. The off-axis phase variance at an angle θ is equal to $(\theta/\theta_M)^{5/3}$. This formula was obtained by assuming that the correction signal applied to each DM is a linear combination of phase screens in all atmospheric layers with suitable weights. The weights are optimized for minimum residual error. Thus, there is no one-to-one correspondence between DMs and turbulent layers or slabs, each DM participates in the correction of the whole atmosphere! Indeed, a better correction is obtained for the layers that are located between the DM conjugation altitudes when corrections are distributed among the neighboring DMs in optimized proportions. A layer outside the DMs conjugation altitude range must be even over-corrected by the nearest DM (i.e. applied to DM with a weight is more than 1), with compensating negative signals applied to other DMs to obtain the perfect on-axis correction (sum of all weights equal to 1).

Parameter θ_M was derived for infinite aperture size and infinite turbulence outer scale. For finite D/r_0, the FOV is larger than θ_M because part of the phase variance is contained in the piston term and does not affect the image quality. Similarly, anisoplanatism is reduced for finite turbulence outer scale. We also considered a more sophisticated algorithm with optimized spatial filtering of phase screens. However, the gains in the FOV size are not dramatic and disappear for large apertures. Thus, θ_M is a good first-order estimate of the correction-limited FOV for OWL.

For one DM conjugated to altitude H_1

$$F_1(h) = |h - H_1|^{5/3}, \tag{2}$$

which reduces to $F_0(h) = h^{5/3}$ if $H_1 = 0$ as in conventional AO. This is the result of Fried.[9] For a two mirror configuration the function has the form:

$$\begin{aligned} 2F_2(h, H_1, H_2) &= |h - H_1|^{5/3} + |h - H_2|^{5/3} \\ &-0.5|H_2 - H_1|^{5/3} - 0.5|H_2 - H_1|^{-5/3}(|h - H_1|^{5/3} - |h - H_2|^{5/3})^2. \end{aligned} \tag{3}$$

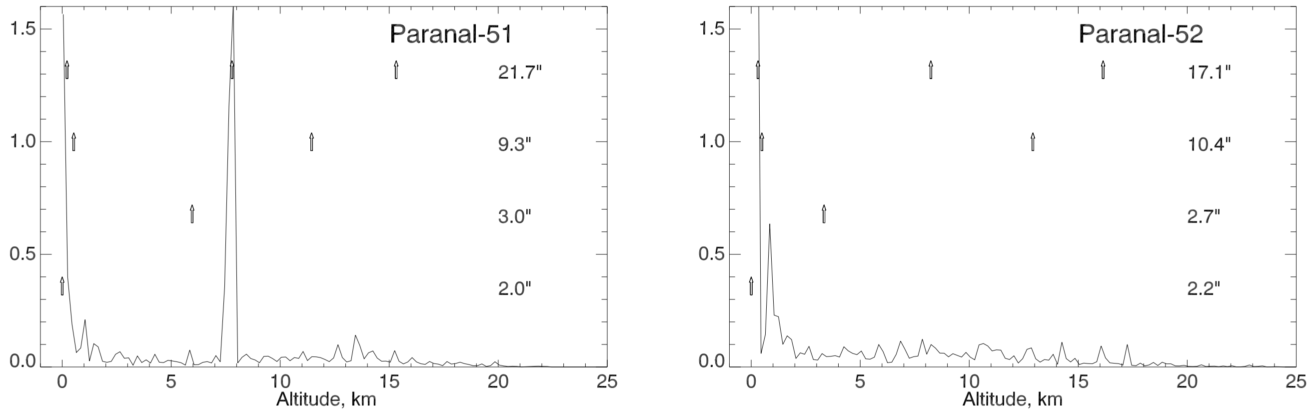

Figure 4. Two representative turbulence profiles at Paranal. Arrows indicate the optimized positions for MCAO configurations with 3 DMs (top row), 2 DMs (middle row) and one DM. Corresponding isoplanatic angles are given on the right-hand side, including the classical θ_0 (the lowest numbers) which correspond to DM in the pupil plane. On vertical axis C_n^2 in the units of 10^{-14} m$^{-2/3}$ is plotted with an altitude resolution of 200 m.

For three or more DMs the expression for F_M is much more complex. The DM conjugation heights H_i were computed with a multi-parameter optimization algorithm to maximize θ_M. We explored also the case when DMs are conjugated to fixed heights, as well as mixed cases, from all H_i fixed to all H_i optimized. For fixed H_i we used the most frequent positions found by height optimization. The values of θ_3 for $\lambda = 500$ nm are given in Table 2.

As can be seen, with 3 DMs conjugated to the optimized heights the FOV gain over θ_0 ranges from 2.6 to 13, with a median of 7.7. If the DMs are conjugated to fixed heights, the gain is lower, but the loss is far from dramatic (gains from 2.2 to 11.8, median 7.2). Thus, it is not really necessary to know the *exact* altitudes of turbulent layers! This good news can be explained by the fact that optimized heights for most profiles are very similar (Fig. 3), with the first DM typically conjugated to 3.4 km, the second one to 10.9 km and the third one to 17.9 km. Optimized conjugate heights of an increasing number of DMs are shown for the two representative profiles in Fig. 4.

Thus, at Paranal the FOV of $\approx 30''$ diameter can be corrected with 3 DMs in the optical, which corresponds to a $3'$ FOV in the K band. Under the best observing conditions the corrected FOV size can be doubled. This FOV is not as large as was believed initially,[13] but still *much* larger than θ_0.

3.3. Effective thickness of the atmosphere

In real life we have to measure the phase perturbations before correcting them. Since the number of turbulent layers is always larger than the number of guide stars, it is not possible to construct and solve a system of linear equations as initially proposed by Tallon and Foy.[6] We can estimate the wavefront coming from the object only in a statistical sense, up to a certain limit. What is this limit?

Ragazzoni et al.[14] performed an experiment to demonstrate that it is indeed possible to estimate the object wavefront by a linear operator applied to the wavefronts of surrounding NGSs. Generally speaking, we look for a best (in the least-squares sense) linear estimator. This resembles Wiener filtering, and the problem is best solved by looking for an optimized filter in the Fourier space.

If only NGS are used for wavefront measurements and if we may neglect the aperture edge effects, each Fourier component of the object wavefront is reconstructed separately from other components. Neglecting also the WFS noise, we obtain the required linear reconstructor as a spatial filter which depends only on the turbulence vertical profile, NGS geometry and object position in the field,[8] but not on the turbulence spectrum.

Wavefront reconstruction will always be good at low spatial frequencies, because they are correlated over large angular distances. It will remain good at high frequencies for a profile composed of a small number of thin layers, with $N_{\mathrm{layers}} < N_{\mathrm{NGS}}$, which corresponds to the tomographic case. For layers of finite thickness, however, the high-frequency wavefront components of the object and all NGS will eventually become decorrelated with each other, making reconstruction impossible. At these frequencies the optimized filter will have a small value. The *error* *transfer function* which describes the fraction of corrected turbulence spectrum will then be equal to 1, while it was close to zero for low spatial frequencies. Integrating the product of the error transfer function and the turbulence spectrum, we estimate the error of object wavefront reconstruction ϵ.

Leaving aside the detailed derivations,[8] we give here the final result only. The variance of the reconstruction error is equal to

$$< \epsilon^2 >= \left(\frac{\Theta \delta}{r_0} \right)^{5/3} e(\vec{\theta}), \tag{4}$$

where Θ is the angular radius of NGS configuration, $\vec{\theta}$ is the source position, $e(\vec{\theta})$ is a function describing the relative error variation across the field, and δ is a new parameter which has a dimension of length and depends on turbulence profile shape and NGS configuration. We call it the *equivalent thickness of the atmosphere.* All error dependence on wavelength is contained in r_0, as typical of many other atmospheric propagation problems.

For a uniform turbulence layer of thickness L, the equivalent thickness $\delta_3 = 0.06L$, $\delta_5 = 0.04L$ for 3 and 5 NGS, respectively. For the mean Paranal profile we obtain $\delta_3 = 875$ m and $\delta_5 = 539$ m. Similar values (889 and 554 m) are obtained for the Hufnagel profile. Even for the Paranal profile 51 with a strong layer, a similar equivalent thickness is obtained (962 and 572 m). Comparing these numbers with a uniform-layer case, we see that they correspond to an overall thickness of the order of 15 km. It means that the reconstruction limit is entirely defined by the large-scale profile features, and is practically insensitive to the layers, contrary to the expectations of earlier works. The extended component of the turbulence profile completely dominates over the layered structure, at least as far as tomographic wavefront reconstruction is concerned.

Our calculations have also shown that the profile *a priori* knowledge needs not be exact. Using the mean Paranal (or even Hufnagel) profiles for the calculation of optimum filters, instead of real profiles, leads to a very small loss of reconstruction quality (δ increases typically by 10%). Hence, the detailed knowledge of the layer structure is of little help. This is in agreement with the other results on NGS tomography.[22]

Taking Θ as the radius of the FOV corresponding to a 1 rad^2 reconstruction error, we obtain from (4) $\Theta = r_0/\delta$, or a $56''$ radius for $r_0 = 0.15$ m and $\delta_5 = 550$ m. The FOV size scales as $\lambda^{6/5}$, leading to a FOV diameter of $11'$ in the K band. Thus, our ability to reconstruct the object wavefront is in fact less restrictive than our ability to correct it with few DMs.

The wavelength dependence of reconstruction and correction errors is the same. It leads to the interesting consideration about the maximum number of pixels in the corrected image. Image size will be of the order of Θ. Pixel size (at Nyquist sampling) must be $\lambda/2D$. The number of pixels along one image axis, $N_{\rm pixel}$, can be estimated as the ratio of those numbers. Taking into account the dependence of r_0 on wavelength, it turns out that $N_{\rm pixel}$ depends on wavelength only weakly:

$$N_{\rm pixel} = \left(\frac{\lambda}{\lambda_0} \right)^{1/5} \frac{2D \, r_0(\lambda_0)}{\delta \, \lambda_0}. \tag{5}$$

Assuming $\delta = 550$ m, $\lambda = 500$ nm, $r_0(\lambda) = 0.15$ m and $D = 100$ m, we obtain $N_{\rm pixel} \approx 110\,000$. For correction-limited FOV (with 3 DMs) $N_{\rm pixel}$ will be 4 times smaller. Going to the wavelength of 2.2 μm increases $N_{\rm pixel}$ by a factor of only 1.34. The conclusion is that the detector format for imaging at a 100 m telescope with MCAO may reach 30x30K.

4. NATURAL GUIDE STARS FOR CORRECTION IN THE INFRARED

It has been proposed[15] to use several NGSs to increase the sky coverage of an MCAO system. If correction only in the near IR is desired, the NGS approach becomes viable in terms of sky coverage. At 1.25 μm $\theta_{\rm M}$ is increased by a factor 3 compared to the visible (see Eq. 1). For $\theta_3 \sim 60''$ in the visible, a $3.6'$-diameter corrected FOV is obtained. The limiting magnitude, as shown by Fig. 1, increases from R $\sim$ 10 to R $\sim$ 13. The sky coverage is plotted in Fig. 5. It shows that with a Strehl ratio of 0.2, SCs of 20%, 65%, 100% are obtained, respectively, at Galactic poles, at average latitudes and at the Galactic disk. For a Strehl ratio of 50%, these numbers become 9%, 35% and 100%. If a 1 magnitude gain in limiting magnitude is obtained compared to a single NGS, the coverages stay roughly unchanged. With a Strehl ratio of 0.5, the SCs become 14%, 53% and 100%, respectively.

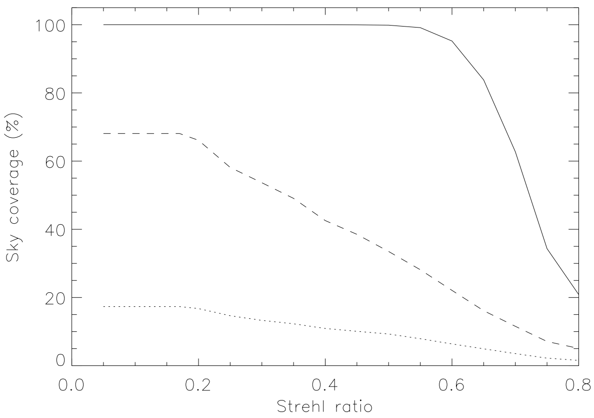

Figure 5. Sky coverage in the J band using 4 NGSs with a corrected FOV of 3′ in diameter. From top to bottom curves: near Galactic plane, average latitude, near Galactic pole.

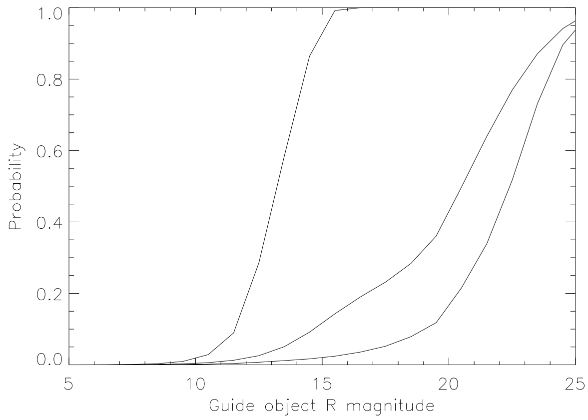

Figure 6. Sky coverage for the 4-LGS case, $\theta_{\rm M} \sim 60'$, top curve to bottom: Galactic disk, average Galactic latitude and Galactic pole.

At 2.2 μm, $\theta_{\rm M} \sim 6'$, the limiting magnitude is about R $\sim$ 15. The sky coverage is then total for all positions in the sky.

5. LASER GUIDE STARS AND CORRECTION IN THE VISIBLE

The LGS approach is not plagued as much by anisoplanatism, since a smaller corrected FOV is needed. However, because the tilt cannot be measured from the LGS, it has been shown[16] that 5 modes have to be measured on a NGS. These modes are tilts, defocus and astigmatism. We therefore propose to use a low-order wavefront sensor (like a curvature sensor) to measure these modes. Since the correction is done in the visible range, the natural reference benefits from the AO correction and the limiting magnitude of the NGS is significantly fainter than on 4-8 m class telescopes. Scaling the current performance of a 19-element curvature sensor, we obtain a limiting magnitude of $\sim$ 23 for a 100 m telescope.[17]

A model of the Galaxy developed by Robin & Crézé 1986 was used to estimate the probability to find a NGS within the corrected FOV. Considering the faint magnitudes this system will be able to use, we also took into account the density of galaxies in the sky. We used galaxy counts given by Fynbo et al. 1999, based on a combination of measurements from the North and South Hubble Deep Fields[20] and the ESO NTT deep field.[21] Near the Galactic pole galaxies become more numerous than stars for magnitudes fainter than $R \sim 22$. A bias may exist since not all of these galaxies can be used as a reference due to their angular size. However, usually, the fainter the galaxies the smaller they are, so this effect should not be significant. We have assumed that galaxies are distributed evenly in the sky. Assuming Poisson statistics, we obtain the probability to find a reference object for a given limiting magnitude.

Fig. 6 yields a SC of 50% at the poles, 80% at average latitudes and 100% near the Galactic plane. Scaling the SR of current curvature systems, we expect a SR between 0.2 and 0.4 for this reference magnitude. At a magnitude of $R \sim 23$, most of the wavefront references sources will be galaxies when observing near the Galactic pole.

6. CONCLUSIONS

Although a realization of an adaptive optical system working with a 100 m telescope in the visible represents a technical challenge due to the large number of DM actuators etc., it is shown here that very large apertures open a number of new possibilities and such a correction becomes feasible for almost any point in the sky. The new approaches involve either use of several widely spaced bright NGS (for a correction in the IR) or a very faint NGS combined with few LGS (correction in the visible). In both cases the correction will be achieved with few DMs conjugated to the optimum heights; in this way the FOV size is increased $\sim$ 10 times compared to the single-DM AO systems, and FOV diameter may reach 1′ in the visible.

ACKNOWLEDGMENTS

This work has benefitted from the European TMR network "Laser guide star for 8-meter class telescopes" of the European Union, contract #ERBFMRXCT960094.

REFERENCES

1. R. Gilmozzi, B. Delabre, P. Dierickx, N. N. Hubin, F. Koch, G. Monnet, M. Quattri, F. J. Rigaut, and R. N. Wilson, "Future of filled aperture telescopes: is a 100-m feasible?," *Proc. SPIE* **3352**, pp. 778–791, 1998.
2. T. Andersen, A. Ardeberg, J. Beckers, R. Flicker, A. Gontcharov, and M. Owner-Petersen, "XLT: The 50 m swedish telescope," in *Proc. of Workshop on Extremely Large Telescopes, Bäckaskog Castle, Sweden, June 1-2*, in press, 1999.
3. M. Mountain, "What is beyond the current generation of ground-based 8-m to 10-m class telescopes and the VLTI?," *Proc. SPIE* **2871**, pp. 597–606, 1997.
4. H. S. Stockman, ed., *The Next Generation Space Telescope - Visiting a time when galaxies were young.* The Association of Universities for Research in Astronomy, Inc., 1997.
5. M. Le Louarn, R. Foy, N. Hubin, and M. Tallon, "Laser guide star for 3.6m and 8m telescopes: performances and astrophysical implications," *Monthly Not. Roy. Astron. Soc.* **295**(4), p. 756, 1998.
6. M. Tallon and R. Foy, "Adaptive telescope with laser probe - isoplanatism and cone effect," *Astron. Astrophys.* **235**, pp. 549–557, August 1990.
7. A. Tokovinin, M. Le Louarn, M. Sarazin, "Isoplanatism in a multi-conjugate adaptive optics system", *J. Opt. Soc. Amer.*, 2000, submitted
8. A. Tokovinin, E. Viard, "Limiting precision of tomographic phase estimation for a large field of view", *J. Opt. Soc. Amer.*, 2000, in preparation
9. D. L. Fried, "Anisoplanatism in adaptive optics," *J. Opt. Soc. Am.* **72**, pp. 52–61, 1982.
10. A. Fuchs and J. Vernin, "Final report on PARSCA 1992 and 1993 campaigns," Tech. Rep. VLT - TRE - UNI - 17400 - 0001, ESO, 1993.
11. M. Azouit and J. Vernin, "Remote investigation of tropospheric turbulence by two-dimensional analysis of stellar scintillation," *J. Atmos. Sci.* **37**, pp. 1550–1557, 1980.
12. M. Sarazin, "Site atmospheric characterization," in *OSA/ESO topical meeting on adaptive optics*, M. Cullum, ed., pp. 439–444, ESO/OSA, 1996.
13. R. Ragazzoni, E. Marchetti, and F. Rigaut, "Modal tomography for adaptive optics," *Astron. Astrophys.* **342**, pp. L53–L56, 1999.
14. R. Ragazzoni, E. Marchetti, and G. Valente, "Adaptive-optics corrections available for the whole sky," *Nature* **403**, pp. 54–56, 2000.
15. R. Ragazzoni, "No laser guide star for adaptive optics in giant telescopes?" *Astron. Astrophys. Suppl. Ser.* **136**, pp. 205–209, 1999.
16. M. Le Louarn and M. Tallon, "3D mapping of turbulence: a solution to the cone effect," *J. Opt. Soc. Am. A*, in preparation, 2000.
17. M. Le Louarn, N. Hubin, M. Sarazin, and A. Tokovinin, "New challenges for adaptive optics: Extremely large telescopes," *Monthly Not. Roy. Astron. Soc.*, submitted, 1999.
18. A. Robin and Crézé, "Stellar population in the Milky Way: a synthetic model," *Astron. Astrophys.* **157**, pp. 71–90, 1986.
19. J. U. Fynbo, W. Freudling, and P. Moller, "Clustering of galaxies at faint magnitudes," *Astron. Astrophys.*, accepted, 1999.
20. R. E. Williams, B. Blacker, M. Dickinson, W. V. D. Dixon, H. C. Ferguson, A. S. Fruchter, M. Giavalisco, R. L. Gilliland, I. Heyer, R. Katsanis, Z. Levay, R. A. Lucas, D. B. McElroy, L. Petro, M. Postman, H.-M. Adorf, and R. Hook, "The Hubble deep field: Observations, data reduction, and galaxy photometry," *Astron. J.* **112**, pp. 1335–1389, 1996.
21. S. Arnouts, S. D'Odorico, S. Cristiani, S. Zaggia, A. Fontana, and E. Giallongo, "The NTT SUSI deep field," *Astron. Astrophys.* **341**, pp. 641–652, 1999.
22. T. Fusco, J.-M. Conan, V. Michau, L. M. Mugnier, G. Rousset, "Phase estimation for large field of view: application to multiconjugate adaptive optics", *Proc. SPIE 3762*, 1999.